Imaging and monitoring with Virtual Sources on a synthetic 3D dataset from the Middle East

Valeri Korneev Lawrence Berkeley National Laboratory; Andrey Bakulin, Jorge Lopez, Shell International Exploration and Production Inc.*

Summary

The Virtual Source (VS) method enables imaging and monitoring below complex and changing overburden. In this study, we apply it to synthetic elastic dataset acquired in deviated observation wells below a 3D model with extremely heterogeneous overburden typical of Middle East fields. Shallow heterogeneity contains both random and regular components in the form of a stack of non-producing layers. While conventional VSP acquisition barely shows any coherent arrivals, the Virtual Source survey reveals high-quality target reflections from producing horizons at depth. Kirchhoff migration of these data perfectly retrieves a simulated time-lapse anomaly.

Introduction

The Virtual Source (VS) method has been proposed by Bakulin and Calvert (2004, 2006) as a practical approach to reduce distortions of seismic images caused by complex overburdens. The method uses data from surface shots and downhole receivers placed below the most complex part of the heterogeneous overburden. The data-driven redatuming technique utilizes downhole recordings to eliminate the transmission effects of the near surface and to obtain reflections from deeper targets, which are free from distortions caused by complex overburden. No knowledge of the velocity model between surface shots and receivers is required. Many Middle East fields suffer from near-surface complexity accompanied by strong vertical velocity gradients and surface topography (Corsten et al, 2005). It is a challenge to obtain any seismic image even for shallow reservoirs of less than 1000 m deep. In recent years, many such reservoirs experienced increased EOR activity due to water or steam floods that demand careful monitoring. Seismic monitoring from the surface is problematic, not only due to imaging issues but also due to near-surface changes that create false 4D responses.

Onshore monitoring with virtual-source seismic in horizontal wells has been offered as a solution in such cases (Bakulin et al, 2007a). Indeed, by placing receivers below the most complex and changing part of the near surface, we can image through the overburden and also eliminate non-repeatability related to any changes occurring above the receivers. While 2D applications have been reported (Bakulin et al., 2007a,b), there is a need to understand a performance of the Virtual Source method in a realistic 3D environment where summation over the area of surface source is performed. Also, areal surveillance requires use of several instrumented wells. Issues such as acquisition design (shot/receiver spacing) of Virtual Source Survey, resolution, as well as sparse imaging of areal VS dataset need to be understood. This is best addressed with a synthetic study that resembles all important features of real data. This study describes the initial part of such an approach. In particular, we focus on describing the model and acquisition geometry, and show initial (2D) results for VS imaging and monitoring using only one of the existing wells. Much more work is planned to develop best practices and extract the full value of Virtual Source monitoring from horizontal wells.

Elastic Earth model

The 3D complex elastic model typical for Middle East reservoirs was created for such studies. The model contains two stacks of layers with 5^o and 15^o dips correspondingly (Figure 1). Immediate near surface (first ~100 m) is very complex, as depicted on Figure 2. The model contains a grid

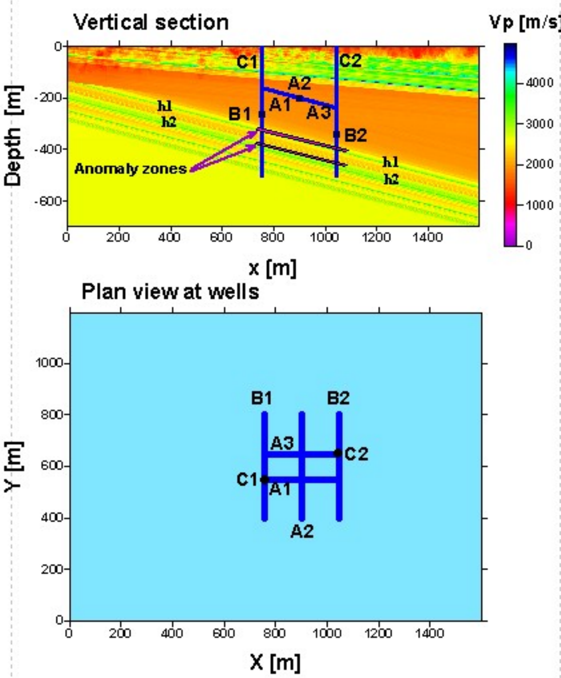

Figure 1. Vertical (upper panel) and plan (lower panel) views on the model and acquisition geometries.

with dimensions 1067 x 801 x 467 that results in ~ 400 million points. Grid spacing is 1.5 m in all directions, which corresponds to 1600 m in x- , 1200 m in y- and 700 m in z- (depth) dimensions. Computations were conducted using 3D finite-difference parallel code developed in Sandia National Laboratory (Symons and Aldridge, 2000).

We did not model any topography of the free surface. In addition, we could not allow very low (realistic) shear velocities to maintain reasonable grid size. To compensate for these effects while still matching the poor quality observed in field data, the decision was made to have somewhat larger (unphysical) contrasts in density values for the near-surface layer (within 0 to 100 m depths). Shallow subsurface heterogeneity was modeled as statistically distributed local scatterers (ellipsoids with both continuous and discontinuous interfaces) with random sizes, orientations and material properties (Figure 2). While not ideal, such a solution led to an increased realistic scattering in the near surface that eventually matched the complexity or “messiness” of the field data (Figures 3, 4), while allowing it to complete the parallel computation of a large dataset in a reasonable time. The heterogeneous model was overlaid by a gradual vertical gradient changing most rapidly at the surface and reaching a constant value at depth.

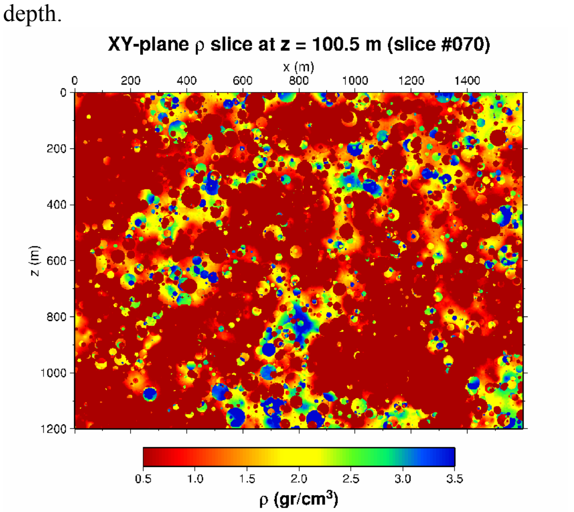

Figure 2. Horizontal slice of density distribution in the 3D model after adding the vertical gradient. Complexity of the shallow subsurface was modeled as a composition of local heterogeneities with statistically distributed geometrical and material parameters.

The base model was used for the generation of a monitor model after introducing local pieces of homogeneous contrasts in oil reservoirs h1 and h2 (Figure 1) in the lower stack of layers, simulating decrease in acoustic impedances caused by steam injection.

Synthetic data set

The computed dataset simulated a large 3D VSP with a rectangular array of 27,354 surface sources. Receivers sit in multiple wells A1, A2, A3, B1, B2, C1, C2 inside the transparent shale layer that is located in the middle of the section below the most challenging part of the section (Figure 1). Since the number of surface sources is far larger than the number of downhole receivers, actual computation was performed using reciprocity, i.e., downhole receivers were turned into sources, whereas surface sources were turned into receivers. Semi-horizontal wells A1, A2 and A3 contain 31, 41 and 31 4C receivers at 10 m spacing, located on a plane parallel to the lower stack of target layers and 200 m above the upper interface of the stack. These wells were designed for data acquisition and processing of Virtual Source Cross-Spread (Bakulin et al, 2007b) using reflected waves. The remaining wells will be used for testing various cross-well configurations with Virtual Source, such as Virtual Cross-Well with reflection data (Bakulin et al., 2007b) for data recorded in wells C1 and C2, and Virtual Cross-Well with head waves or refracted arrivals (Tatanova et. al, 2007) using data from wells B1 and B2. The 3C surface sources are on a 7.5 m grid and cover essentially the entire surface of the model.

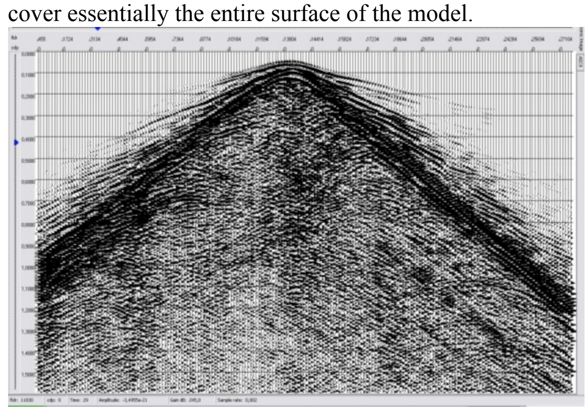

Figure 3. Receivers gather at 200 m depth from an array of surface sources along the line y=600m. Source is a vertical force; shown is the vertical component of displacement at one of the receivers inside well C1. Note that it is hard to see any coherent arrivals. For synthetic surface seismic data, the situation is even worse because waves pass heterogeneous subsurface layers twice.

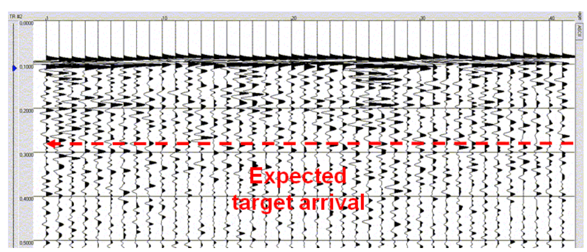

Figure 4. Walk-above VSP with surface shots and downhole receivers in well A2. Expected target arrival at 270 ms (red) is unrecognizable on data.

The source waveform was a Delta-function. The output traces have 1024 data samples at 2 ms intervals. Before processing, the traces are convolved with a chosen wavelet with maximum frequency not exceeding 100 Hz to avoid artifacts caused by numerical dispersion. The dataset requires 500 Gb for data storage and allows many possibilities for 3D tests of the Virtual Source method. In this study, we present the processing results only for a single vertical section along well A1. The anomaly zones which are intersected by this traverse have -9% P-wave impedance contrast in the layer h1 and -15% impedance contrast in the layer h2 (Figure 1).

Virtual Source data

Due to the reciprocal way of computing data (with downhole sources), we also obtained the “ground truth” dataset with actual sources in place of Virtual Sources. This dataset allows comparison of virtual with real downhole sources. Figure 5 shows such comparison for well A1 when VS summation goes over limited aperture right above the well.

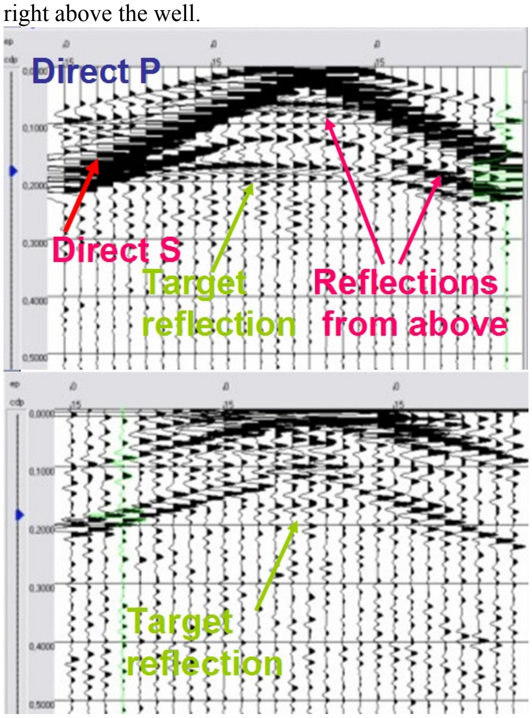

Figure 5. Comparison of synthetic real-source-gather (upper panel) and Virtual-Source gather (lower panel) for real/Virtual source location at station 17 of well A1. VS data is obtained by cross-correlation of vertical components from vertical-force sources at the surface. Direct arrivals are clipped on real source data to emphasize reflections. Note strong reflections from the free surface which are visible for real-source traces. These reflections interfere with waves coming from the target layer below.

Real-source traces are dominated by direct waves and waves reflected from above and represent strong noise when trying to image the structure below. In contrast, the predominantly downward radiation pattern of the Virtual Sources (Bakulin and Calvert, 2006) largely eliminate these unwanted arrivals. Cross-correlation of the wavefield gated in first arrivals with the ungated datasets feeds the Virtual Source with downgoing energy, thus eliminating reflections from above. This preferred directivity can be further enhanced by a proper choice of summation aperture. This emphasizes waves propagating in a desired near-vertical direction by summing over the surface sources in the vicinity of stationary points (Snieder et al., 2006) located at intersections of prolonged desired ray paths with integration surface. More revealing, the effect of Virtual Source directivity can be seen on Figure 6, where zero-offset 2D images are shown along A1, A2 and A3 wells.

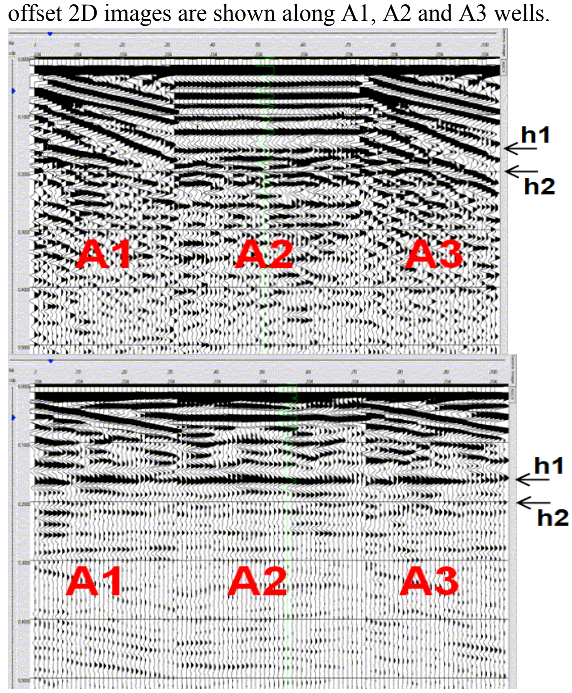

Figure 6. Zero-offset images along A1, A2 and A3 wells for synthetic real-source gather (upper panel) and Virtual-Source gather (lower panel). Virtual-Source gather reveals clear arrivals from target horizons h1 and h2.

Imaging VS and VSP data using receivers from well A1

VS data were generated using cross-correlation of vertical components and summation over the surface aperture of source inside the box 600m < x < 1200m, 300m < y < 700 m. Synthetic data allowed a reliable automatic picking of the first arrivals. The VS data set comprised 31 VS gathers for all 31 receivers, totaling in 961 traces. The data were subject to a Kirchhoff migration using same average velocity models for baseline and monitor models. Similar migration was done for the real-source data. Figure 7 shows the comparison of migration results. Virtual Source migration image is clearly much better than the one obtained using real-source data. The distortions on the real-source image appear due to strong reflections from above caused by close upper-stack and subsurface heterogeneities. These unwanted waves strongly interfere with target reflections, bringing high amplitude artifacts into the final image.

We may speculate that dual-sensor wavefield separation on real-source data may remove reflections from above (Mehta et al, 2007). However, presence of random scatterers in the near-surface is likely to degrade the quality of such separation. Noticeably, migrated image of Virtual Source data is somewhat biased to lower frequencies, which is the result of squared source wavelet in VSM that can be removed by deconvolution. Source wavelet used in computations has the maximum at 40 Hz while the highest frequency reaches 90 Hz.

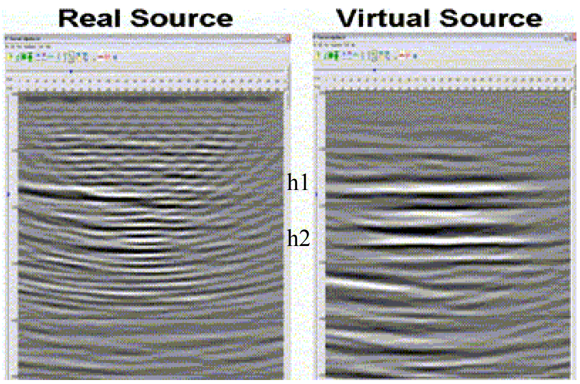

Figure 7. Comparison of migrations using downhole datasets with real and Virtual Sources. VS image reveals clear target reflections that are practically invisible on a real-source migration.

Even better results are obtained when imaging is applied to the differences between baseline and monitor VS data (Figure 8). VS migration result is practically free of artifacts, except for some additional reflections below the anomaly zones caused by uncorrected time-shifts due to velocity decrease in reservoir layers. Figure 9 shows amplitude distribution along the images of layers h1 and h2 on Figure 8b. The ratio between image amplitudes corresponds to the actual contrast differences which were used in the monitor model (Figure 8a). Nonuniform amplitudes along the layers are caused by edge effects in acquisition geometry.

Discussion and conclusions

We presented synthetic examples of Virtual Source imaging and monitoring to a complex 3D elastic dataset resembling a typical Middle Eastern field. Despite strong 3D near-surface heterogeneity, areal summation of cross-correlations leads to greatly improved VS images as compared to actual downhole sources or horizontal VSP. 4D anomalies are reliably recovered by migrating the difference in VS dataset.

Future studies will focus on assessing effects of up-down separation (Mehta et al, 2007), correcting radiation patterns of the Virtual Sources (van der Neut, 2008), obtaining an

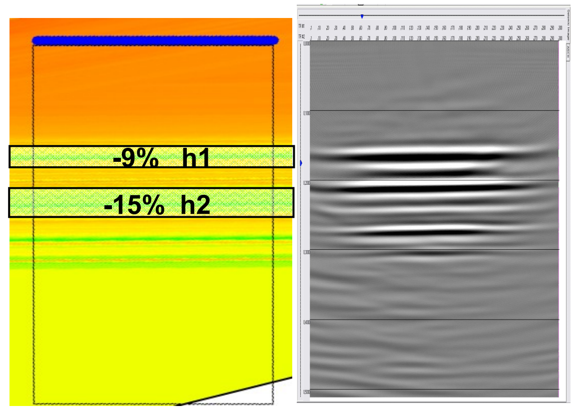

Figure 8. Rotated by 15° velocity model for the target stack of layers (left panel) with shown anomaly zones. Migrated image (right panel) of the VS difference data between the baseline and monitor datasets. Clearly visible are time-lapse differences for the layers containing anomaly zones.

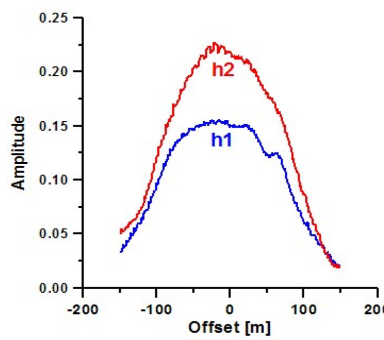

Figure 9. Amplitude of differential image from right panel of figure 6 computed along the anomalous layers h1 (blue line) and h2 (red line). Note that amplitude ratios are consistent with anomaly contrasts.

areal image using multiple wells (cross-spreads) and mapping areal 4D anomalies in a more quantitative fashion. In addition, best practices for acquisition geometry needs to be evaluated. Proper 12C dataset (3C sources and 4C receivers) also allows for the testing of a multicomponent version of the Virtual Source Method.

Acknowledgments

We thank Dave Aldridge, Nate Gaunt and Neil Symons (all at Sandia National Laboratory) for performing the synthetic seismic modeling. We are grateful to Albena Mateeva (Shell) for valuable suggestions.

EDITED REFERENCES

Note: This reference list is a copy-edited version of the reference list submitted by the author. Reference lists for the 2008 SEG Technical Program Expanded Abstracts have been copy edited so that references provided with the online metadata for each paper will achieve a high degree of linking to cited sources that appear on the Web.

REFERENCES

Bakulin, A., and R. Calvert, 2004, Virtual source: New method for imaging and 4D below complex overburden: 74th Annual International Meeting, SEG, Expanded Abstracts, 2477–2480.

———2006, The virtual source method: Theory and case study: Geophysics, **71**, SI139–SI150.

Bakulin, A., J. Lopez, A. Mateeva, and I. S. Herhold, 2007a, Onshore monitoring with virtual-source seismic in horizontal wells: Challenges and solutions: 76th Annual International Meeting, SEG, Expanded Abstracts, 2893–2897.

Bakulin, A., A. Mateeva, K. Mehta, P. Jorgensen, J. Ferrandis, I. S. Herhold, and J. Lopez, 2007b, Virtual source applications to imaging and reservoir monitoring: The Leading Edge, **26**, 732–740.

Corsten, C., S. Mahrooqi, and P. Engbers, 2005, Good vibrations in Fahud: The Leading Edge, **24**, 827–830.

Mehta, K., A. Bakulin, J. Sheiman, R. Calvert, and R. Sneider, 2007, Improving the virtual source method by wave-field separation: Geophysics, **74**, V79–V86.

Snieder, R., K. Wapenaar, and K. Larner, 2006, Spurious multiples in seismic interferometry of primaries: Geophysics, **71**, SI111–SI124.

Symons, N., and D. Aldridge, 2000, 3D elastic modeling of salt flank reflections at Bayou Choctaw Salt Dome, Louisiana: 70th Annual International Meeting, SEG, Expanded Abstracts, 2436–2439.

Tatanova, M., A. Bakulin, B. Kashtan, and V. Korneev, 2007, Head-wave monitoring with virtual sources: 77th Annual International Meeting, SEG, Expanded Abstracts, 2994–2998.